

Nonstructural Components and the Rainflow Counting Algorithm

Christa Kelleher
Lafayette College

REU Host Institution: University at Buffalo
REU Faculty Advisor: Gilberto Mosqueda
PhD Mentor: Rodrigo Retamales

Abstract:

The purpose of this research was to update current protocols for imposing and inducing motion on various displacement sensitive and acceleration sensitive nonstructural components. These components, which include suspended ceilings, light fixtures, elevators, piping systems, and heating-ventilation-air-conditioning (HVAC) systems, account for 75% of building construction costs and a large portion of damage during earthquakes. Using real floor motions obtained from the CSMIP database, the instrument time histories for both displacement and acceleration were used as input to Matlab functions, which applied the rainflow cycle counting algorithm to the data. For estimation of cycles imposed on displacement sensitive objects, the 84th percentile floor response spectrum for the number of cycles greater than 10% of the maximum cycle range and the number of cycles greater than 50% of the maximum cycle range. To find the number of cycles induced in acceleration sensitive objects, the period of the secondary system was compared to the number of cycles greater than both 10% and 50% of the maximum cycle range. For both acceleration and displacement counting estimations, Matlab plots were created to represent the large number of time history inputs and statistically analyze the range of data. The protocol, once updated, will be applied to the Nonstructural Component Simulator (NCS) at the University of Buffalo earthquake laboratory. The NCS will eventually be used to test a full-scale hospital room, allowing for seismic design and testing of hospital equipment.

Introduction

Nonstructural components are building components that are nonessential to the structure of the building, but provide much needed building functions. They include suspended ceilings, light fixtures, elevators, piping systems, and heating-ventilation-air-conditioning (HVAC) systems. Nonstructural building contents include everything from bookshelves and cabinets to water pumps and computers. An area of expanding research, nonstructural component and building content damage comes at a high cost. It has been estimated that 75% of the construction cost of buildings is tied to non-structural components. Such damage also poses a risk to human health both directly and by preventing evacuation.

Nonstructural component research has emerged at the University of Buffalo through the use of the Nonstructural Component Simulator (NCS), a piece of equipment which has the ability to simulate floors in a building. The eventual goal of the NCS is to use it in the testing of nonstructural components.

The NCS runs off of a protocol, which is a series of frequencies supplied to the hydraulics which control the floor motions. The primary focus of current research is the development of these protocols to serve both acceleration sensitive and displacement sensitive equipment testing.

Objectives

The research objective was to estimate the number of cycles imposed on both acceleration sensitive and displacement sensitive equipment, including inputs from a range of building types, earthquakes, and floors. The number of cycles estimated would be used to create a new protocol for the NCS.

Research Approach

The research approach was to first identify information to analyze, create the programs for analysis, run the programs, and then examine the results and draw appropriate conclusions. These steps are each described in greater detail below.

Information

The CSMIP Database is comprised of approximately 70 buildings. To select buildings for analysis, the coordinates of each of the buildings were used to estimate the distance between the earthquake epicenters and the buildings. All buildings outside of a distance of 35 kilometers from any earthquake's epicenter were immediately ruled out. This amounted to a selection of 14 buildings. For each of the 14 buildings, the following variables were considered for selection:

- Design date
- Number of stories
- Building use
- Site geology

- Earthquake record
- Building material and structure
- Fundamental period
- Peak ground acceleration (PGA)

Information was compiled in an Excel spreadsheet, and used to select 6 buildings for study. A wide range of buildings was included. The six buildings selected are displayed in Figure 1. A description of each follows.

Building 24464:

Building 24464 is a 20 story hotel located in North Hollywood, CA. The structure is made up of reinforced concrete columns and beams, and was built in 1967. Site geology can be characterized as sandstone and shale. The earthquake record used is from the Northridge earthquake, which had an epicenter at a distance of 15 kilometers from the building. The building period was estimated to be 2.56 seconds, and the peak ground acceleration (PGA), 0.3 g.

Building 24322:

Building 24322, located in Sherman Oaks, CA, is 13 stories high. Built in 1964 and currently serving commercial use, it is a distance of 13 kilometers from the epicenter of the Northridge earthquake. Building material includes concrete slabs, beams, and columns. Site geology is alluvium. The PGA is 0.75 g and the period is 0.836 seconds.

Building 24514:

Building 24514 is a hospital located in Sylmar, CA, approximately 13 kilometers from the epicenter of the Northridge earthquake. It was built in 1976, overlaying alluvium geology. The building consists of concrete slabs, a metal deck, and steel frames. It is six stories high, and has a PGA of 0.8 g and a period of 0.402 seconds.

Building 24386:

Building 24386 is a seven story hotel building in Van Nuys, CA. Site geology is alluvium. The sensor records come from the Northridge earthquake, with an epicenter at a distance of 7 kilometers from the building. The building was built in 1965, and consists of concrete slabs and columns, as well as spandrel beams. The PGA was recorded at 0.45 g and the building period is 1.575 seconds.

Building 47459:

Building 47459 is located in Watsonville, CA. Sensor records are from the Loma Prieta earthquake, with an epicenter at a distance of 17 kilometers from the building. The building is four stories tall, and is used for commercial purposes. It consists of concrete

slabs and shear walls, and site geology is fill over alluvium. The PGA is 0.58 g and the building period is 0.366 seconds.

Building 24629:

Building 24629 is located in Los Angeles, CA, at a distance of 32 kilometers from the epicenter of the Loma Prieta earthquake. The building was designed in 1988, and consists of 54 stories. It is an office building with a recorded PGA of 0.13 g and a period of 6.2 seconds. Site geology is alluvium over sedimentary rock. The building's structure consists of concrete slabs and steel frames and decking.

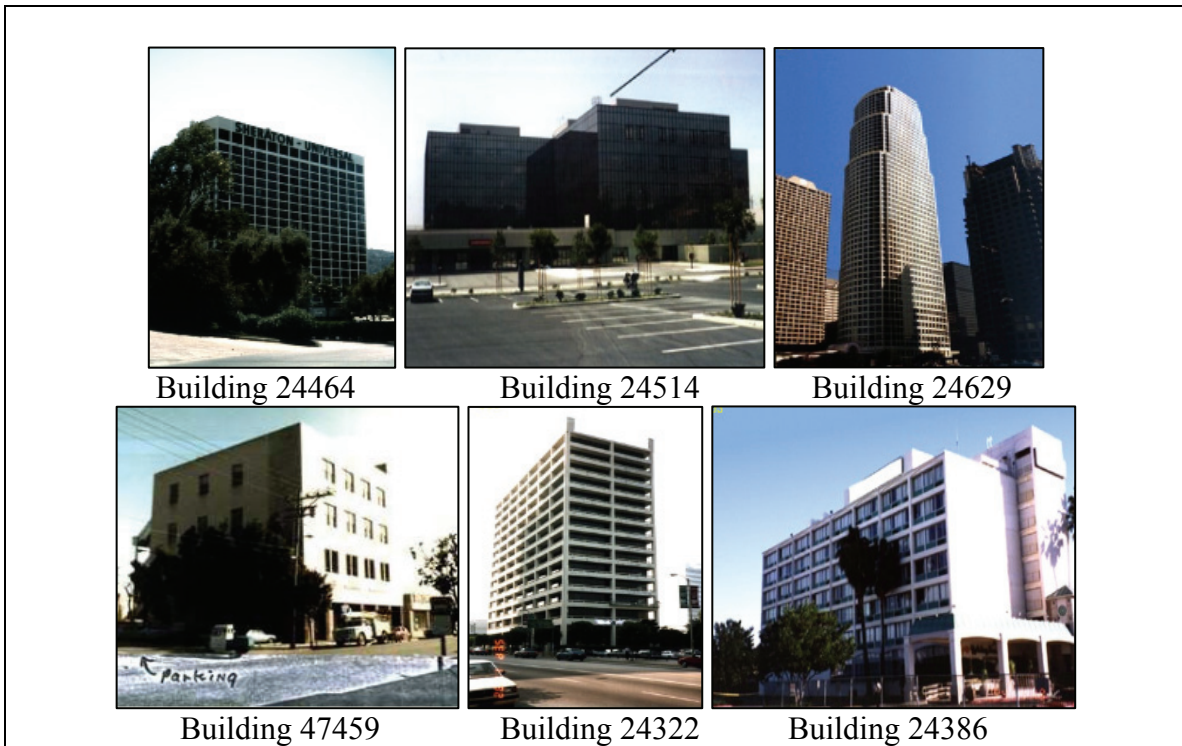


Figure 1: Buildings Selected from the CSMIP Database

Linear Interpolation

The CSMIP database utilizes two interpolation schemes to compute interstory drift histories. The first is cubic spline interpolation, based on the equation:

Where $f(h)$ is a response parameter, such as displacement, and h represents the elevation of the floors to which the response parameters were recorded for. The second interpolation scheme used by the database is linear interpolation. Far more simplistically, linear interpolation utilizes equation (1) below:

$$f(h) = h*c + d. \quad (1)$$

A system of two equations can be solved for a floor between two instrumented floors. For a given time step, the variables $f(h)$, displacement, and h , floor height, are known for the two instrumented floors. The variables c and d were solved for using the system of two equations. Then, the interstory time history was solved for using the known height, h , and the values of c and d . New time histories were generated by programs created in matlab. Interstory drift was found by subtracting the displacement time history of one floor from another. Since linear interpolation was used, it was unimportant whether

Drift Histories

In buildings where story heights were distributed evenly, interstory drift histories were calculated for each adjacently instrumented floor. Drift histories were always calculated between sensors located in a similar position in the x-y plane. The drift histories calculated for each building are described below.

Building 24464:

Story heights were evenly distributed for 20 floors. Interstory drift histories were calculated and analyzed between the ground floor and first floor, the first floor through the seventh floor, the seventh floor through the 14th floor, and the 14th through the 20th floor. Sensors 1, 2, 3, 4, 5, 6, 7, 8, and 9 in the north-south direction and sensors 10, 11, 12, 13, and 14 in the east-west direction were analyzed. A total of 12 drift histories were created.

Building 24322:

Excluding the first floor, story heights were evenly distributed for the 13 floors. Interstory drift histories were calculated and analyzed between the ground floor and first floor, the first floor through the seventh floor, and the seventh floor through the 13th floor. Sensors 2, 3, 5, 6, 8, 9, 11, and 12 in the north-south direction and sensors 1, 4, 7, and 10 in the east-west direction were analyzed. A total of nine drift histories were created.

Building 24514:

A total of six interstory drift histories per sensor pair and direction were calculated, corresponding to the ground floor through the sixth floor. Sensors 3, 5, 7, 8, and 9 in the north-south direction and sensors 10, 11, 12, and 13 in the east-west direction were analyzed. A total of 14 drift histories were created.

Building 24386:

A total of seven interstory drift histories per sensor pair and direction were calculated, corresponding to the ground floor through the seventh floor. Because of consistent story heights, drift histories between floors two through five were the same. Sensors 1, 3, 4, 6,

7, 8, and 14 in the north-south direction and sensors 9, 10, 11, 12, and 13 in the east-west direction were analyzed. A total of 16 drift histories were created.

Building 47459:

A total of four interstory drift histories per sensor pair and direction were calculated, corresponding to the ground floor through the fourth floor. Sensors 5, 6, 7, 8, 9, and 10 in the north-south direction and sensors 11, 12, and 13 in the east-west direction were analyzed. A total of 12 drift histories were created.

Building 24629:

Story heights for the 54 story building were relatively evenly distributed. I calculated and analyzed interstory drift histories between the ground floor and 20th floor, the 20th floor through the 36th floor, the 36th floor through the 46th floor, and the 46th through the 54th floor. Sensors 7, 9, 10, 12, 13, 14, 16, 17, 19, and 20 in the north-south direction and sensors 6, 8, 11, 15, and 18 in the east-west direction were analyzed, and a total of 11 drift histories were created.

The Rainflow Algorithm

To ensure that the rainflow program was operating correctly in Matlab, the rainflow output was first compared to a hand calculation of the rainflow function. Once the two were deemed to be the same, the Matlab function was implemented for analysis. To apply the Rainflow algorithm

To filter the time histories, two Matlab programs were used. First 'sig2ext' – designed by Adam Niesony - is applied to the data to find extrema. While the program filtered out most of the excess data, it filtered the data so that local minimums or maximums were captured between absolute minimums or maximums. I created the program 'minmaxex' to further filter out these local extrema points. Between these two programs, the loading histories were filtered such that a maximum always followed a minimum, and a minimum, a maximum. This is critical for the application of the Rainflow algorithm. Although counting yielded both full cycles and half cycles, both were considered to be the same in analysis.

The Rainflow algorithm output data listed each cycle excursion, the cycle amplitude, and the average cycle value. The important values when considering Rainflow values are the number of cycles and the corresponding range, which was found to be twice the amplitude. These two variables were considered for statistical analysis.

Rainflow Applications to Displacement Data

For the displacement analysis, Rainflow was only applied to the calculated drift histories.

Rainflow Applications to Acceleration Data

For acceleration analysis, Rainflow was applied to the calculated response from the equation of motion for a single degree of freedom system. The equation of motion was simplified using Newmark’s Method, and the acceleration history used for input. The equation of motion used is shown in equation (2) below:

$$f(t) = m\ddot{x} + c_v\dot{x} + kx$$

$$\ddot{x} = \text{acceleration} \tag{2}$$

$$\dot{x} = \text{velocity}$$

$$x = \text{displacement}$$

For equation 2, mass (m) is held constant. The other input into this equation is the secondary period, which was varied from 0 to 5 seconds at increments of 0.1 seconds. The equation was solved for each acceleration history for the varied secondary periods, amounting to 52 records per acceleration history. Matlab programming was used to solve the equation and tabulate the results.

Statistical Analysis of Calculations

Statistical calculations were performed on the tabulated data for both displacement and acceleration analysis. Matlab was first used to tabulate the number of cycles with ranges greater than 10, 20, 30, 40, 50, 60, 70, 80, and 90% of the maximum cycle excursion per time history. For this data corresponding to each time history, the mean, standard deviation, and 84th percentile values were calculated for channel groupings. These included North-South channels, East-West channels, and all channels. The statistics were calculated using Matlab, for which the functions of mean and standard deviation were predefined. The 84th percentile value is the sum of the mean and a single standard deviation.

Displacement Analysis

The 84th number of cycle excursions for North-South, East-West, and all channels appear below in tables 1, 2, and 3.

Table 1: North-South Channels – 84th Number of Cycle Excursions

% of A _{max}	0	0.1	0.2	0.3	0.4	0.5	0.6	0.7	0.8	0.9
No. of Cycles	201	46	31	22	16	12	8	6	4	3

Table 2: North-South Channels – 84th Number of Cycle Excursions

% of A _{max}	0	0.1	0.2	0.3	0.4	0.5	0.6	0.7	0.8	0.9
No. of Cycles	167	45	37	29	23	19	13	8	6	4

Table 3: North-South Channels – 84th Number of Cycle Excursions

% of A _{max}	0	0.1	0.2	0.3	0.4	0.5	0.6	0.7	0.8	0.9
No. of Cycles	189	46	33	25	19	15	10	7	5	3

The percentage of the maximum cycle excursions that are of statistical significance are the 10th percentile value and the 50th percentile value. For the North-South channels, 46 cycles had ranges greater than 10% of the maximum cycle excursion, and 12 cycles greater than 50% of the maximum cycle excursion. For East-West channels, these values were 45 and 19 cycles, correspondingly. When all of the channels were evaluated, the 10th percentile value was 46 and the 50th percentile value was 15.

To better display the data, figure 2 below shows the plotted curves for the percentage of the maximum cycle excursion for all channels, separated by buildings. Each color corresponds to one of the six buildings processed:

- Building 24514 – Green,
- Building 24386 – Yellow,
- Building 24464 – Cyan,
- Building 24322 – Magenta,
- Building 24629 – Blue, and
- Building 47459 – Red.

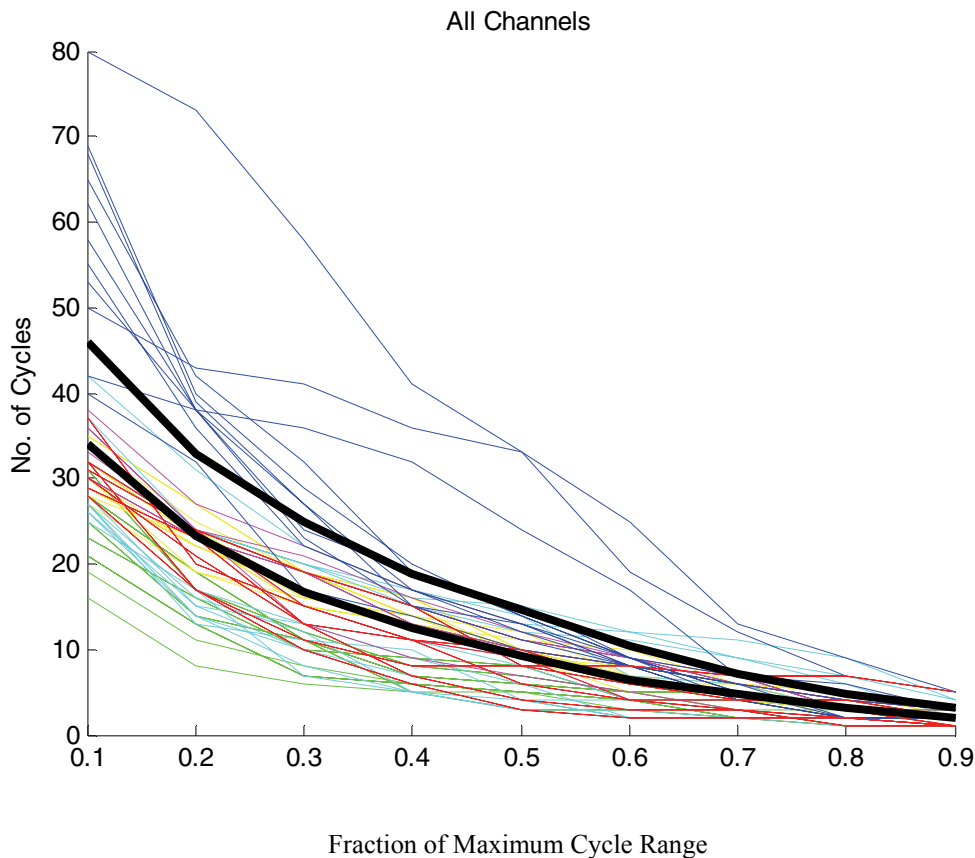


Figure 2. Displacement Analysis, Color-Coded by Building

Figure 3 displays all of the channel data in green, with the mean number of cycle excursions shown by the green line and the 84th percentile number of cycle excursions shown by the red line.

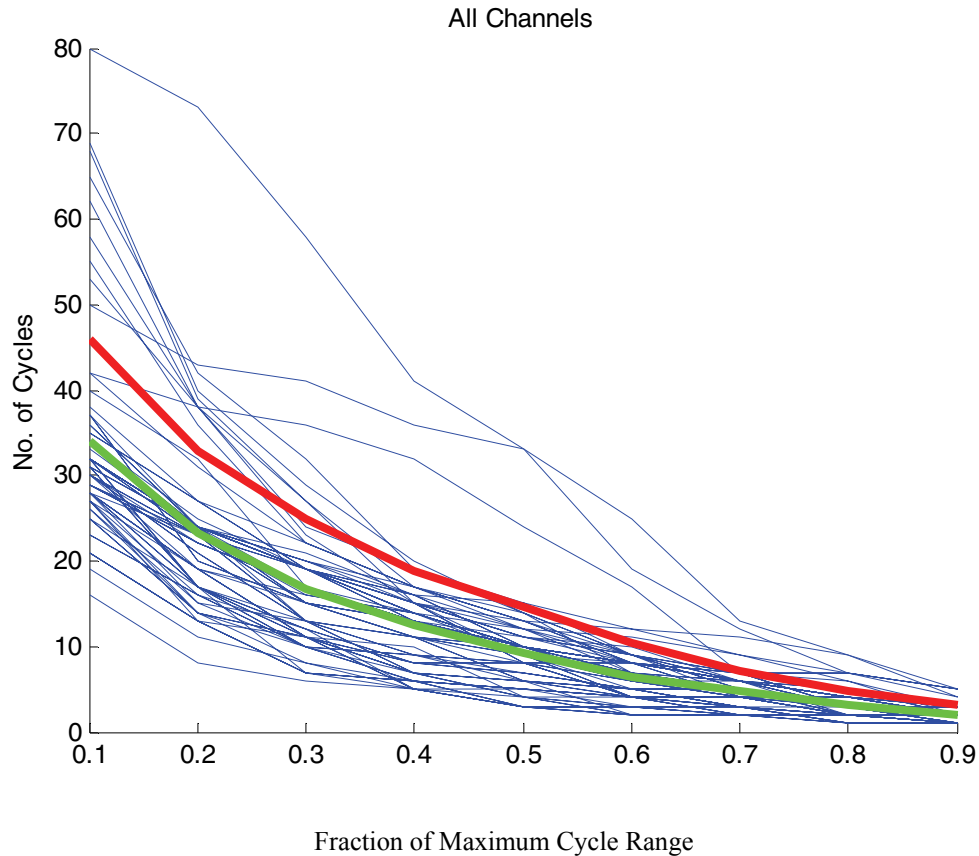


Figure 3. Displacement Analysis, with Mean and 84th Percentile Data

Acceleration Analysis

The acceleration analysis yielded slightly different results than the displacement analysis. For each of the secondary period calculations, Matlab was used to determine the number of cycles greater than 10% of the maximum cycle excursion for each channel. The same calculations were performed for the number of cycles greater than 50% of the maximum cycle excursion. Thus, there are 84th percentile values for each secondary period evaluated. These appear in tables 4 and 5 below.

Table 4: 84th Number of Cycle Excursions with $R > 0.1R_{10}$

Period (secs)	0	0.1	0.2	0.3	0.4	0.5	0.6	0.7	0.8	0.9	1
No. of Cycles	651	182	109	75	61	55	49	48	39	41	42
Period (secs)	1.1	1.2	1.3	1.4	1.5	1.6	1.7	1.8	1.9	2	2.1
No. of Cycles	41	50	44	44	42	43	42	41	43	47	45
Period (secs)	2.2	2.3	2.4	2.5	2.6	2.7	2.8	2.9	3.0	3.1	3.2
No. of Cycles	45	44	44	45	48	49	50	49	50	48	46
Period (secs)	3.3	3.4	3.5	3.6	3.7	3.8	3.9	4	4.1	4.2	4.3
No. of Cycles	46	44	44	40	39	39	39	38	38	38	38
Period (secs)	4.4	4.5	4.6	4.7	4.8	4.9	5.0				
No. of Cycles	38	38	39	39	41	43	41				

Table 5: 84th Number of Cycles Excursions with $R > 0.5R_{10}$

Period (secs)	0	0.1	0.2	0.3	0.4	0.5	0.6	0.7	0.8	0.9	1
No. of Cycles	292	134	90	65	55	48	41	39	36	39	36
Period (secs)	1.1	1.2	1.3	1.4	1.5	1.6	1.7	1.8	1.9	2.0	2.1
No. of Cycles	35	40	36	38	39	41	39	36	37	40	39
Period (secs)	2.2	2.3	2.4	2.5	2.6	2.7	2.8	2.9	3.0	3.1	3.2
No. of Cycles	37	38	36	36	39	41	41	40	40	39	37
Period (secs)	3.3	3.4	3.5	3.6	3.7	3.8	3.9	4.0	4.1	4.2	4.3
No. of Cycles	36	35	36	33	33	34	34	34	34	34	34
Period (secs)	4.4	4.5	4.6	4.7	4.8	4.9	5.0				
No. of Cycles	33	33	32	34	37	38	38				

The data can be further displayed in graphical form. The data was processed for both 10% and 50% of the maximum cycle ranges, plotting the number of cycles versus the secondary system period. The data is displayed correspondingly in figures 4 and 5 below.

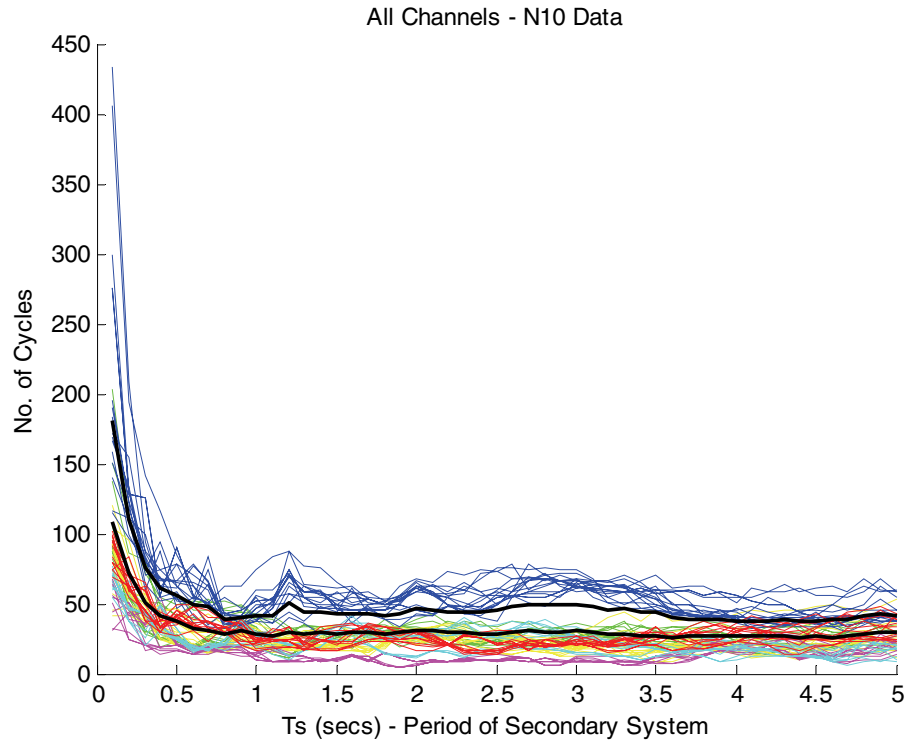


Figure 4. Number of Cycles for 10% of the Maximum Cycle Range versus the Secondary System Period

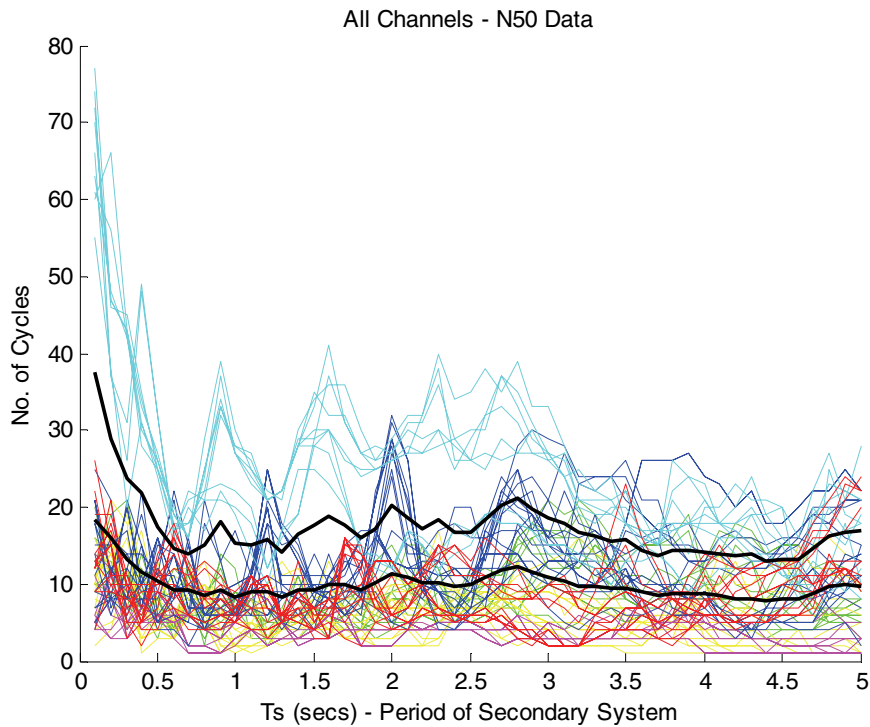


Figure 5. Number of Cycles for 50% of the Maximum Cycle Range versus the Secondary System Period

Applications and Future Work

The acceleration and displacement analysis has applications for the qualification and testing of building components on the Nonstructural Component Simulator (NCS), an equipment piece at the University of Buffalo Earthquake Laboratory. The number of cycle excursions is used to create the protocol that determines the movement of the hydraulics on the NCS. The conversion from the number of cycles imposed and secondary period of the system to the protocol will be done by graduate student Rodrigo Retamales, using mathematical transformations.

While the data for the protocol was generalized using six buildings from different earthquakes, more records could be obtained and processed to average the number of cycles imposed over a greater range of data inputs. The goal of the protocol is to generalize the number of cycles imposed by earthquakes in a variety of buildings, so the greater the number of inputs, the more finely tuned the protocol will be.

In a greater sense, the next steps for this research is to create the new protocol for the calculated number of cycles imposed and to test it on various acceleration sensitive and displacement sensitive equipment. The future of nonstructural component research will inevitably supply many more applications and areas of research for the NCS and the University of Buffalo Research Laboratory.

Acknowledgements

This research would not have been possible without funding from NSF for the REU program, or the organization provided by the MCEER staff, specifically Sofia Tangalos. In addition, the advising of graduate student Rodrigo Retamales was vital to project completion. Professor Gilberto Mosqueda also was integral in project development and explanations of the scope of work to be performed.

References

- CSMIP Instrumented Building Response Analysis and 3-D Visualization System TECHNICAL MANUAL*. John A. Martin & Associates. 2005.
- Miranda, E. and Reinoso, E. "Estimation of floor acceleration demands in high-rise buildings during earthquakes." *The Structural Design of Tall and Special Buildings*. 14, 2, 2005, 107-130.
- Mosqueda, G., Retamales, R., Filiatrault, A., and Reinhorn, A. "Testing Facility for Experimental Evaluation of Nonstructural Components Under Full-Scale Floor Motions."